HITACHI

GE Hitachi Nuclear Energy

Richard E. Kingston
Vice President, ESBWR Licensing

PO Box 780 M/C A-55
Wilmington, NC 28402-0780
USA

T 910 675 6192
F 910 362 6192
rick.kingston@ge.com

Proprietary Notice
This letter forwards proprietary information in accordance with 10CFR2.390. Upon the removal of Enclosure 1, the balance of this letter may be considered non-proprietary.

MFN 08-659

Docket No. 52-010

September 04, 2008

U.S. Nuclear Regulatory Commission

Document Control Desk
Washington, D.C. 20555-0001

Subject: Response to NRC Request for Additional Information – Related to ESBWR Design Certification Application – RAI Number 21.6-44 Supplement 1

The purpose of this letter is to submit the GE Hitachi Nuclear Energy (GEH) response to the U.S. Nuclear Regulatory Commission (NRC) Request for Additional Information (RAI) sent by NRC email. GEH response to RAI Number 21.6-44 Supplement 1 is addressed in Enclosures 1, 2 and 3.

Enclosure 1 contains GEH proprietary information as defined by 10 CFR 2.390. GEH customarily maintains this information in confidence and withholds it from public disclosure. Enclosure 2 is the non-proprietary version, which does not contain proprietary information and is suitable for public disclosure.

The affidavit contained in Enclosure 3 identifies that the information contained in Enclosure 1 has been handled and classified as proprietary to GEH. GEH hereby requests that the information in Enclosure 1 be withheld from public disclosure in accordance with the provisions of 10 CFR 2.390 and 10 CFR 9.17.

If you have any questions or require additional information, please contact me.

Sincerely,

Richard E. Kingston

Richard E. Kingston
Vice President, ESBWR Licensing

D068
NRO

Enclosures:

1. MFN 08-659 – Response to NRC Request for Additional Information – Related to ESBWR Design Certification Application – RAI Number 21.6-44 S01 – GEH Proprietary Information
2. MFN 08-659 – Response to NRC Request for Additional Information – Related to ESBWR Design Certification Application – RAI Number 21.6-44 S01 – Non-Proprietary Version
3. MFN 08-659 – Response to NRC Request for Additional Information – Related to ESBWR Design Certification Application – RAI Number 21.6-44 S01 – Affidavit

cc:	AE Cubbage	USNRC (with enclosure)
	RE Brown	GEH/Wilmington (with enclosure)
	DH Hinds	GEH/Wilmington (with enclosure)
	eDRF	0000-0058-1420/1

Enclosure 2

MFN 08-659

Response to NRC Request for Additional Information

Related to ESBWR Design Certification Application

RAI Number 21.6-44 S01

Non-Proprietary Version

NRC RAI 21.6-44 S01

This RAI is related to qualification of the boron mixing model in TRACG. The staff needs additional information to determine that the test cited is applicable to ESBWR conditions. The staff is concerned that there is no test data to verify the mixing behavior of the SLCS system as injected into the core bypass. The tests cited to be applicable to the ESBWR are those where the boron is injected through the HPCS sparger for a scaled BWR/5 and 6. The justification used is predicated on knowing the ESBWR boron flow path and that it is similar to that of the HPCS sparger location. However this leads to a circular reasoning since the data is supposed to be used to inform the TRACG model that it is adequately calculating the boron mixing and flow paths in the core. Do you have any test data that verifies that injection of boron into the core bypass periphery will have mixing and flow paths similar to that of the HPCS sparger? In the RAI response, the scaling was only performed for the radial and axial directions and not as rigorous as that was done for the SBWR where you scaled such parameters as boron injection concentration, temperatures, loss coefficients, etc. Please provide a more rigorous scaling analysis. In addition, comparing the mixing tests to the ESBWR MSIV closure ATWS event seems awkward. The ESBWR MSIV closure ATWS event is so dissimilar to the experiment that a direct comparison would be difficult. Are there any comparisons using a TRACG04 input deck of the same experiment? The staff would like additional information about the test conditions. Please provide the following reference used in the RAI response: Test Report Three-Dimensional Boron Mixing Model, General Electric Co., Proprietary Information, NEDE-22267, Class III, October 1982 (RAI response reference 21.6-44-3).

GEH RESPONSE

The previous response to RAI 21.6-44 [5] was centered on the comparison of boron mixing measurements from a scaled BWR/5 facility with TRACG04 predictions of boron mixing for an ESBWR ATWS event. The BWR/5 experiments in Reference [1] that were selected in the original response [5] as most representative of the ESBWR ATWS event add boron to the core through the HPCS sparger ring at the top of the fuel assemblies. Currently, no TRACG04 predictions of the experiments have been carried out: however, an earlier version of TRACG has been validated against experiments [0]. In the current response, it will be shown that selected BWR/5 experiments are appropriate for assessing the accuracy and conservatism of boron mixing predictions of the ESBWR during the ATWS scenario of interest.

A high fidelity, transient, Computational Fluid Dynamics (CFD) prediction was performed simulating the mixing of sodium penta-borate solution in the bypass spaces of the ESBWR during the MSIV closure ATWS event. The CFD model was performed as an alternate calculation to the TRACG04 prediction (Reference [3]) and as such, has been created to be back-to-back with the TRACG04 model: in terms of the region modeled (model domain), initial and boundary conditions, fluid properties, etc. The CFD predictions presented in this response show very good agreement with the Tests 342 and 345 selected in the original response [5]. This agreement verifies both the accuracy of the CFD and the similarities of boron mixing that occur in the BWR and

ESBWR configurations. Additionally, the CFD predictions are used to identify the conservatism in the TRACG04 prediction of boron mixing and, thus, core shutdown time.

Also, scaling comparisons of the selected BWR/5 experiments and the ESBWR ATWS scenario have been performed in detail as part of this response. These comparisons show that the experiments and ESBWR are similar to one another when appropriately normalized, in terms of the mechanisms that transport boron through the bypass spaces.

This RAI response follows the following outline:

1. APROPRIATENESS OF EXISTING TEST DATA: The selected test data from Reference [1], and used in the response to RAI 21.6-44 [5], is shown to be representative of the boron mixing in the ESBWR core during the ATWS MSIV closure event of interest. Also included is a discussion on the appropriate scaling between the BWR/5 simulation in the Vallecitos test facility [1] and the ESBWR for boron transport in the bypass region.
2. CFD MODEL OVERVIEW: The details are presented of a high fidelity, transient, Computational Fluid Dynamics (CFD) prediction of the mixing of sodium penta-borate in the bypass spaces of the ESBWR core during the ATWS event.
3. VALIDATION OF CFD PREDICTIONS WITH EXISTING TEST DATA: The level of accuracy of the CFD predictions is identified via comparisons between the ESBWR CFD prediction and the existing BWR/5 test data.
4. CFD PREDICTIONS VS. TRACG04 PREDICTIONS: CFD and TRACG04 predictions for the ESBWR boron mixing are compared directly, to demonstrate the conservatism of the TRACG04 results.
5. CONCLUSIONS. Based on the results of item 1 through item 4 listed above, conclusion are drawn to cover the concerns in this RAI question.

1. APPROPRIATENESS OF EXISTING TEST DATA

The response to RAI 21.6-44 S0 describes the selection of experiments from [1] that are most representative of the ESBWR ATWS transient. The tests selected are numbers 332, 342, and 345, defined in [1] on Page 2-99. Tests 342 and 345 are used in the current response. Reference [1] has been provided to the NRC as part of this response (per request).

The Vallecitos test facility, [1] is at [[ ]] geometric scale to a BWR/5. The operational parameters of the test facility (flow rates, etc.) were set by matching the correct non-dimensional performance of the real BWR reactor. Because of the differences between the ESBWR ATWS event and the transient events investigated in the test facility, the scaling between the two is revisited to ensure appropriateness in the comparison of results. All supporting calculations used in this section are presented in Appendix A, including nomenclature definitions and references.

The original scaling of the operating point of the test facility to match the BWR/5 reactor is described in Reference [1], Page 2-2, and is based on matching a modified Froude number between the test facility and the BWR. The Froude number is the ratio of the buoyant forces acting to the inertial content of the flow. The Froude number is defined below as:

$$(1) \qquad FR = \frac{(\rho_{SLCS} - \rho_{BULK})\, g\, L_{FR}}{\rho_{BULK}\, V_{Bypass}^{\ 2}} = \frac{g(\gamma_{SLCS} - 1)L_{FR}}{(V_{Bypass})^2} = \left(\frac{\text{Buoyancy Force}}{\text{Intertial Content}}\right)$$

where L_{FR} is an appropriate length scale representative of the distance over which density gradients exist. In Equation 1, the quantities ρ_{SLCS}, ρ_{BULK}, γ_{SLCS}, and g are defined in Appendix A, while V_{Bypass} and L_{FR} are defined as below.

<u>VELOCITY SCALE</u>: For the ATWS event of interest, boron transport processes in the bypass spaces are caused primarily by the removal of fluid from the bypass space and into the fuel bundles through the leakage holes positioned at the lower tie plate. Of secondary importance is the addition of SLCS fluid to the bypass spaces: however, the ratio of SLCS to Leakage volumetric flow rates (RQ) is less than [[ ]] for the three cases considered here (See Table 1 for Values). An appropriate convection velocity scale in the bypass spaces is defined as the total leakage flow rate through all lower tie plate leakage holes, divided by the axial cross-section area of the bypass spaces.

$$(2) \qquad V_{Bypass} = \frac{Q_{Leakage-total}}{A_{Bypass}} = \frac{A_{Leakage-Total} \cdot V_{Leakage}}{A_{Bypass}}$$

Where V_{Bypass}, $Q_{Leakage-Total}$, $A_{Leakage-Total}$, $V_{Leakage}$, and A_{Bypass} are defined in Appendix A. The V_{Bypass} definition of Equation (2) is interpreted as follows: the total leakage flow exiting the bypass can be thought of as a sink of fluid from the bottom of the core; uniformly distributed over the core cross-section. Therefore, A_{Bypass} is the appropriate choice for defining the flow area. While the local velocities at the leakage holes can be [[ ]] times greater than V_{Bypass} (see VR values in Appendix A), the V_{Bypass} value definition of Equation (2) is most representative of the transport processes throughout the entire bypass space.

For the ESBWR case, the leakage velocity was determined using a representative $\dot{m}_{Leakage}$ (see Appendix A for its definition) taken from the TRACG04 solution. For the test facility, the vapor content in the fuel bundles is simulated through the injection of air near the core plate at a known flow rate. Special measurements of the discharge coefficient for the lower tie plate leakage holes in the test facility were carried out and reported in [1, Section 2.4], and used to define a procedure for determining the leakage flow rate as a function of air flow rate to the bundles. This procedure was used here to define V_{Bypass} for the experimental tests.

<u>LENGTH SCALE</u>: The appropriate length scale for defining the Froude Number of Equation 1 (L_{FR})is the axial (i.e., vertical) distance over which the buoyancy forces act in the bypass space. This length is the elevation difference between the highest axial

location of SLCS addition to the bypass space and the bottom of the bypass space (i.e., the top of the core plate).

For the BWR configurations of Tests 342 and 345, the SLCS fluid enters the core bypass spaces through a simulated HPCS ring sparger positioned axially above the waterline. The ring sparger deposits SLCS fluid onto the waterline: hence, the waterline elevation is the highest axial location. For the ESBWR configuration, the highest SLCS injector nozzle is situated at an elevation of [[ ]] above the top of the core plate, which is roughly half of the overall bypass space height. The injector nozzles are oriented in the radial-tangential plane and do not introduce any SLCS fluid to elevations above the highest-most injector nozzle.

FROUDE NUMBER: The Froude number calculations for the Test 342, Test 345, and ESBWR operations are provided in Appendix A. The calculated values of Froude numbers are provided in Table 1. The Froude number of the ESBWR ATWS event is closer to that of Test 345 than of Test 342: hence, Test 345 data is expected to be most representative.

RATIO OF VOLUME FLOW RATES: Table 1 also identifies the ratio of volume flow rates (RQ) for Test 342, Test 345, and ESBWR ATWS: defined in Equation 3.

(3)
$$RQ = \frac{Q_{SLCS}}{Q_{Leakage-total}}$$

Table 1 shows that the ESBWR ATWS RQ value is within 3% of the value for Test 345, and is more than twice the value for Test 342. Therefore, Test 345 is once again most representative. However, the RQ values in Table 1 are less than 8% for all three cases, indicating that the dominant cause of convective transport in the bypass space is the leakage flow into the fuel assemblies.

Table 1: Froude Number Comparisons between ESBWR and Experimental Tests

Case	Velocity Scale: (V_{Bypass})	Length Scale: (L_{FR})	SLCS Specific Gravity: (γ_{SLCS})	Froude Number: (FR)	Ratio of Vol. Flow Rates: (RQ)
ESBWR	[[				
Test 342					
Test 345					]]

2. CFD MODEL OVERVIEW

A brief description of the CFD model is provided here. A further-detailed description can be found in [2]. Previous transmittal to the NRC [3] included portions of the CCL file text (i.e., an exported text file that describes the CFD model's boundary conditions), and answers to specific questions raised about the model by NRC reviewers. Additionally, the NRC has informally requested the volume of the CFD model vs. elevation, and this information has been provided here, in Appendix B.

The CFD model domain consists of a 1/8 azimuthal sector of the ESBWR reactor core: between the top of the Core Plate and the bottom of the Top Guide. The model domain was limited to the bypass spaces only. The CFD model included much of the three-dimensional geometry associated with the fuel bundles and control blade handles present near the core plate. The proper SLCS injector nozzle geometry of the ESBWR core is included in the CFD model. Boron enters the core bypass region from the SLC system injector nozzles.

The CFD model was created and solved using the ANSYS Workbench suite of commercial CFD tools. The geometry of the ESBWR for the CFD model domain was read from formal design documents and created directly in ANSYS Design Modeler CAD software. The total size of the model mesh was 25 million nodes (solution points). For comparison, the TRACG04 model nodalizes the entire ESBWR core bypass space with approximately 100 nodes.

CFX-Pre was used for pre-processing and model set-up. The CFD model domain matches axial and radial node locations of the TRACG04 model. To facilitate a direct comparison between the two models, time-dependent inlet and exit boundary conditions for the CFD model were extracted directly from the TRACG04 analysis of ATWS MSIV closure event (Refs. [4], [6], [3]). The extracted boundary conditions include the total pressure and total temperature at the top opening of the model, the inlet mass flow rate and temperature at the SLCS injector jets, and the exit mass flow rates at the fuel assembly leakage holes. The fuel assembly leakage holes were simulated in the CFD model, with each hole tagged to match the corresponding fuel assembly grouping in the TRACG04 model.

The fluid in the CFD model was treated as liquid water with properties defined using ASME-1967 tables.

The Unsteady, Reynolds-Averaged Navier Stokes (URANS) equations were solved over the model domain using CFX-Solve. Turbulence closure terms in the URANS equations were modeled using the Shear Stress Transport (SST) two-equation turbulence model. Inlet boundary conditions for the two turbulence equations (turbulent kinetic energy and turbulent specific dissipation rate) were unknown, and values were assumed based on 5% turbulence intensity and a turbulent-to-molecular viscosity ratio of 10.

To model the mixing of sodium penta-borate with water in the model, it was assumed that the fluid was locally a homogeneous mixture of SLCS fluid and pre-existing core fluid, sharing a common momentum and energy solution. Numerically, this was accomplished by solving the single-fluid Navier-Stokes equations, plus an additional passive scalar transport equation for the SLCS fluid mass fraction (B). Boundary conditions for the passive scalar transport equation were B=0 at the top inlet, B=1 at the SLCS injector jet inlets, and zero gradient at walls and exits. Further details on the passive scalar approach to modeling boron mixing can be found in [2].

The CFD model solution was performed as a transient solution beginning at an appropriate initialization. To initialize the flow, the steady-state solution was first solved with the boundary conditions from TRACG04 at the instant the SLCS injector flow was initiated (Time = 188.7 Seconds). The transient solution was then performed using 2nd order upwind discretization of the time derivatives and a physical timestep size of 0.1 seconds. One hundred seconds of transient solution was performed. This corresponds to the time in the TRACG04 solution where the sodium penta-borate begins to spill over the top of the fuel channels and the CFD model does not account for this, and is no longer a valid comparison with TRACG04.

Post-processing of the transient solution results was performed using CFX Post. The process of looping over the solution timesteps, loading the timestep's results files, post-processing the instantaneous results, and outputting the desired information was automated using the integrated replay files and PERL scripting language features of CFX-Post.

3. COMPARISONS OF ESBWR PREDICTIONS WITH TEST DATA

To simultaneously judge the accuracy of the CFD prediction and the similarity of SLCS mixing between BWR and ESBWR configurations, the CFD and TRACG04 results were compared with the measurement data from Test 342 and Test 345 of Reference [1]. Comparisons are made in the form of a Mixing Coefficient vs. Time. The Mixing Coefficient is defined as the ratio of the local concentration of SLCS fluid to the global-average concentration of the total SLCS fluid accumulated in the vessel. Note that in the experiment, SLCS fluid mixing was simulated as thermal mixing between cold and hot water. The appropriateness of comparing species mixing with thermal mixing is discussed in page 2-8 of Reference [1].

To facilitate comparisons between the two configurations, axial and radial measurement locations in the experiment were normalized, and equivalent normalized locations determined for the ESBWR geometry. An illustration of the geometry normalization is provided in Figure 1. Predicted mixing coefficient values were averaged over the tangential direction. Parameters shown in Figure 1 such as Z_{TCP}, Z_{BTG}, Z_{INJ4}, R_{Shroud} are defined in Appendix A; R_{Inner}, R_{Outer}, Z_{AN1} and Z_{AN2} are described below.

The radial location was normalized as the fraction of radial distance to the core shroud. In the current response, comparisons between the experiments and predictions are made at two measurement points in the test facility: R_{Inner} = [[ ]] and R_{Outer} = [[ ]]. The equivalent locations in the ESBWR geometry are R_{Inner} = [[ ]] and R_{Outer} = [[ ]] when the same fractions of the total radius were used as in the test.

The axial location from the experimental facility was normalized as the fraction of the total elevation difference between the bottom of the top guide and the top of the core plate. This normalization is illustrated as AN1 in Figure 1. The normalized axial location from the experiment was [[ ]]. This normalized value was then used to determine the corresponding axial location for the ESBWR predictions in two ways:

described as "AN1" and "AN2" in Figure 1. The two ESBWR axial locations are at (Z_{AN1} – Z_{TCP}) = [[ ]]and (Z_{AN2}- Z_{TCP}) = [[ ]] above the top of the core plate.

The CFD model results were interrogated at both Z_{AN1} and Z_{AN2} locations for comparison with the data from the experimental facility. Z_{AN1} represents an equivalent normalized location based on the geometric height of the core, while Z_{AN2} represents an equivalent normalized location based on the highest point of SLCS fluid entry. The two locations bound the problem of how to identify an appropriate equivalent axial normalized location between the ESBWR & BWR/5 configurations, given their dissimilarity in SLCS entry point. Note, however, that in the TRACG04 model, the same computational node encompasses both Z_{AN1} and Z_{AN2}.

In Figure 2, the TRACG04 and CFD mixing coefficient results are compared with measurements from Test 342 and Test 345. CFD predictions at both Z_{AN1} and Z_{AN2} are shown. Parts (A) and (B) of Figure 2 show comparisons at R_{Inner} and R_{Outer} locations, respectively. Time values in Figure 2 are offset to be zero at the time of SLCS flow initialization.

Reference [4, Page 82] describes the blockage added to the TRACG04 solution between the outer and middle rings of the bypass space (first conservatism), in order to inhibit the propagation of boron toward the center of the core and, thus, add conservatism to the TRACG04 prediction of core shutdown time. This blockage exists in the TRACG04 model at a radial location between R_{Inner} and R_{Outer}.

Figure 2 shows that differences between the two experiments and the two axial-normalized locations in the CFD results are most significant through the first 50 seconds of transient time. At the R_{Outer} location, the two CFD prediction curves are within 20% of the Test 345 data (i.e., that which scaled most similarly to the ESBWR) as early as 25 seconds into the transient, and continue that agreement throughout the prediction time interval. Similar agreement is shown at the R_{Inner} location for the AN2 CFD prediction curve, while the AN1 curve shows closer agreement with the Test 342 data. After 50 seconds of transient, all CFD prediction curves and test data are within 20% of each other. The agreement between the CFD predictions and experimental data serves to validate both (a) the accuracy of the CFD model and (b) the similarity between the ESBWR ATWS event and the test data. Additionally, the agreement between the data from Tests 342 and 345 beyond the first 50 seconds of transient indicates that the dependency of boron transport on FR and RQ becomes weak in these times.

In contrast, the TRACG04 model results in Figure 2 conservatively deviate from the data by 100% or more at both R_{Inner} and R_{Outer}. The TRACG04 model shows the accumulation of SLCS fluid in the outer radial locations (i.e., outside the ring blockage) and almost non-existent SLCS fluid in the inner radial locations. As a reference, the TRACG04 solution's predicted time from SLCS initialization to core shutdown is reported in [4, Appendix 2, Table 21.6.8.1, Page 151] as [[ ]] after the SLCS flow is initialized), with very little change in reactivity present before time 240 seconds (i.e., the first 50 seconds of transient after SLCS flow is initialized), as shown in [4, Figure 8.1.10, Page 89].

Equivalent Locations between Vallecitos & ESBWR

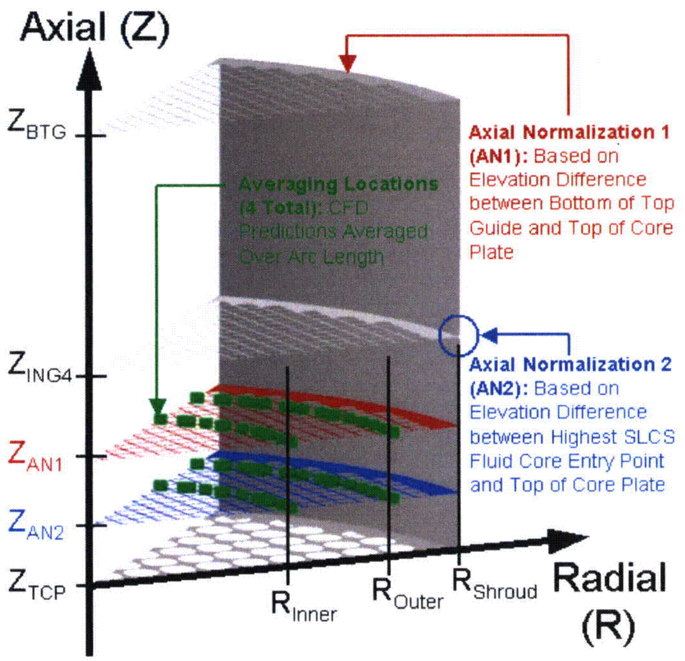

Vallecitos Experiment:

- Datasets 342 and 345 Deemed Most-Representative of the ESBWR ATWS Event of Interest
- Mixing coefficient values were derived from measurements at two radial locations (Inner and Outer) and two axial locations (Higher and Lower)

Location Normalization:

- Match Normalized Axial (Z) and Radial (R) Locations between ESBWR CFD Model & Vallecitos Experiment
- Radial Normalization using the Core Shroud Inner Diameter
- Two Alternatives for Axial Normalization: **AN1** & **AN2** (see left for definitions)
- Line-Average the CFD Solution in the Tangential Direction (over **GREEN** lines at left)

Figure 1: Normalization of Locations between ESBWR and BWR/5 Test Geometries

[[

]]

Figure 2: Comparisons of Mixing Coefficient Prediction Results (ESBWR ATWS Event) with Test Measurements (BWR/5 Scaled Experiment)

4. CFD PREDICTIONS VS. TRACG04 PREDICTIONS

To assess the CFD predictions of boron mixing in the core bypass spaces versus the TRACG04 predictions, two different Figures of Merit (FOM's) were used for comparing the CFD and TRACG04 results. FOM1 is the total mass of boron present in a particular portion of the bypass space. FOM2 is the time-aggregate mass of boron that has passed through the fuel assembly leakage holes for selected groupings of fuel assemblies. In the absence of boron spillover from the top of the fuel assemblies, FOM2 represents the total amount of boron that has accumulated in the fuel assemblies, which will be transported upward by the boiling flows within the fuel assemblies and eventually will spill over the top of the assemblies. Since the SLCS inlet mass flow boundary condition for the CFD model was extracted directly from the TRACG04 solution, the global quantity of boron at any transient time shown here is equal to the sum of FOM1 and FOM2, and is the same between the CFD and TRACG04 models.

In the nodalization of the TRACG04 model, the various fuel assemblies are grouped together as inner, middle, outer, or peripheral assemblies: based on their proximity to the core centerline. Figure 3(A) shows the extents of these four groupings as they exist in the CFD model. The bypass space in the TRACG04 model is nodalized in annular-shaped nodes, or Rings, as illustrated in Figure 3(B). FOM predictions from the TRACG04 model therefore naturally exist for the nodal definitions of Figure 3: namely, FOM1 values for bypass space rings Inner, Middle, and Outer, and FOM2 values for fuel assembly groupings Inner, Middle, Outer, and Peripheral.

The post-processing of FOM values from the CFD results was performed in such a way so as to be consistent with the nodalization of the TRACG04 model. For example, the CFD prediction of FOM1 for the bypass space middle ring was determined by volume integrating the local solution of boron mass per unit volume over the annular space between radial bounds of [[ ]] and [[ ]], shown in Figure 3(B). Also as example, the CFD prediction of FOM2 for the middle fuel assemblies was determined by time-integrating the total leakage flow rate of boron exiting the bypass spaces into the leakage holes of the middle assembly grouping shown in Figure 3(A). Note also that the FOM values derived from the CFD results were scaled by a factor of 8, to account for the 1/8 sector of the CFD model domain and make the values representative of an entire core.

Figure 4 shows plots of FOM1 versus transient time, compared between CFD and TRACG04 for the Inner, Middle, and Outer annular regions of the bypass space (defined in Figure 3(B)). Figure 4(A) shows FOM1 values for TRACG04 axial node levels 4 through 8. These nodes extend axially from the top of the core plate (= bottom of CFD model) to the top of the active fuel in the fuel assemblies. Figure 4(B) shows FOM1 values for TRACG04 axial node level 4 only. TRACG04 axial node 4 extends from the top of the core plate to the bottom of the active fuel. The TRACG04 axial nodalization of the bypass space is illustrated in [4, Figure 8.1.1, Page 87]. There is no radial blockage for node 4 in the TRACG model and the SLCS fluid in this node can communicate radially, and with leakage holes in the proximity.

In both Figure 4(A) and 4(B), the TRACG04 solution shows essentially zero boron present in the inner and middle rings, and significantly more boron accumulating in the outer and peripheral rings. At [[ ]] seconds, Figure 4 shows that the CFD model stops accumulating boron in the bypass spaces and appears to reach a nearly steady state, while the TRACG04 model continues to accumulate boron in the bypass spaces.

Figure 5 shows plots of FOM2 versus transient time for the CFD and TRACG04 solutions. The TRACG04 results show negligible boron entering the inner and middle fuel assemblies until about 240 seconds, when the middle fuel assemblies begin to show some boron accumulation. The CFD results show boron beginning to accumulate in the inner and middle fuel assemblies at approximately time [[ ]] seconds, respectively. For fuel assemblies in all rings, the CFD results show higher accumulation of boron in the fuel assemblies. The CFD results also show a much more uniform distribution of boron in fuel assemblies at various radial locations, indicating a more effective poisoning of the entire core than what is predicted with TRACG04.

The differences between the CFD and TRACG04 results are due to a combination of the obvious differences in modeling methodology, and the less-obvious differences in model resolution. For the same boron mass in the same bypass space volume (i.e., equivalent FOM1), the CFD nodalization will resolve the local highs and lows in boron concentration, whereas the TRACG04 nodalization will see a much more homogeneous mixture over the same volume. In reality, the SLCS fluid accumulates near the core plate, resulting in higher localized boron concentrations in the vicinity of the fuel assembly leakage holes. The CFD resolution captures this stratification and, thus, ingests a higher fraction of SLCS fluid into the fuel assembly leakage holes. For the CFD model, the flow rates of SLCS fluid entering and exiting the model domain equalize at a time of [[ ]] seconds, and the FOM curves of Figures 4 and 5 show a fairly steady state (i.e., flat-line for FOM1, constant slope for FOM2).

Note that in both Figures 4 and 5, various indicators of boron spillover times, predicted by the TRACG04 model, are provided. The boron spillover in the TRACG04 plot is due to the boron mass ingested into the fuel assemblies via the lower tie-plate leakage holes being transported upward via the boiling flows within the fuel assemblies. Upon reaching the top of the fuel assembly, the boron spills back over into the bypass space, where it is again subjected to buoyant and convective transport mechanisms. Since the flow in the fuel assemblies and boron spillover is not modeled in the CFD model, but is modeled in the TRACG04, the spillover time indicators are used to gauge the time period during which TRACG04 vs. CFD comparisons are appropriate.

Appendices C and D present contour images of local SLCS fluid mass fraction (B) predictions from the CFD results at different 2D-planar locations in the core. Time snapshots are shown at every 5 seconds through the transient prediction. The locations of the 2D-planar images are illustrated at the top of each page.

Appendix C shows contour images of SLCS fluid mass fraction in Radial-Axial planes at various angular locations from the plane of the SLCS injectors. In the first [[ ]] seconds of transient, SLCS fluid is seen to migrate both axially downwards and radially inwards at the same time. By Time = [[ ]] seconds, the contours have reached a stable state: that is, while small fluctuations in the contour levels continue to occur, the overall magnitudes and shapes of the contours are very similar between time snapshots. This finding is consistent with the flattening of the FOM1 curves in Figure 4, and the constant slope of FOM2 curves in Figure 5. The image sequences of Appendix C also clearly show the stratification of SLCS fluid toward the bottom of the core, due to its higher density. Likewise, SLCS fluid is not transported to axial elevations above the highest injector nozzle.

Appendix D shows contour images of SLCS fluid mass fraction in the Radial-Tangential plane, at various axial elevations. The stratification of SLCS fluid toward the lower elevations is again visible, when comparing the image sequences between the different elevations. The high contour levels near the core plate are indicative of the fraction of SLCS fluid in the fuel assembly leakage flow exit boundary condition. The image sequences in Appendix D also show very little variation in boron levels in the tangential direction after Time = [[ ]] seconds, with the exception of the peripheral portion of the bypass space near the SLCS injectors.

[[

]]

Figure 3: TRACG04 Model Nodalization Description

[[

]]

Figure 4: Predictions of Boron Mass in the Bypass Spaces (FOM1)

[[

]]

Figure 5: Predictions of Boron Mass in the Fuel Assemblies (FOM2)

[[

]]

Figure 5 (cont.): Predictions of Boron Mass in the Fuel Assemblies (FOM2)

5. CONCLUSIONS

Based on the Froude Number (FR) and Volume Flow Rate Ratio (RQ) calculations and comparisons presented in Section 1, it is concluded that the use of the existing test data (Ref. [1], Tests 342 and 345) is appropriate for assessing the accuracy and conservatism of boron mixing predictions of the ESBWR during the ATWS scenario of interest. Specifically, Test 345 is most representative of the ESBWR ATWS event.

Based on the level of agreement between CFD predictions and the measurements from BWR/5 Tests 342 and 345 presented in Section 3, and the FR & RQ scaling arguments presented in Section 1, it is concluded that the CFD model is an adequately accurate representation of the boron transport through the bypass space during the ESBWR transient, so as to be used to judge the conservatism in the TRACG04 prediction of boron mixing (and hence, core shutdown time).

Based on the comparisons of Section 4, between prediction results from the artificially blocked TRACG04 model and the validated CFD model, it is concluded that the TRACG04 model's prediction of boron mixing through the ESBWR core is conservative compared with the CFD model, which has been validated as representing reality (per Section 3). The conservatism of the TRACG04 model exists in that boron is artificially inhibited from entering the inner [[ ]] of the core's radial extent and forced to pool in the outer [[ ]]. Therefore, boron poisoning of reactivity in the core is severely limited in the inner radial locations. Since the TRACG04 model's core shutdown time prediction is a direct result of the model's prediction of boron propagation into all regions of reactivity in the core, the core shutdown time predictions from the TRACG04 model are also conservative.

Additionally, the elevation difference between the SLCS injectors and the top of the active fuel assemblies, and the greater weight of the SLCS fluid vs. the bulk fluid in the core (which causes it to sink), results in the absence of boron in the bypass spaces above the elevation of the highest injector nozzle, for both TRACG04 and CFD models. The SLCS instead relies on the transport of boron into the fuel assemblies through the lower tie-plate leakage holes, and the subsequent transport of boron upwards by the boiling two-phase flow within the assemblies to effectively poison the higher elevations of active fuel in the core. This mechanism for boron transport is also severely limited in the TRACG04 model for the inner and middle fuel assemblies, as shown by the FOM2 comparisons in Figure 5. The inhibited boron transport into and through the inner and middle fuel assemblies is due to the artificially-imposed blockages, and thus represents added conservatism to the TRACG04 prediction of core shutdown time.

REFERENCES

[0] NEDC-32725P, Vol. 2, "TRACG Qualification for SBWR", Section 5.4., September 1997

[1] "Test Report Three-Dimensional Boron Mixing Model," General Electric Co., *Proprietary Information*, NEDE-22267, Class III, October 1982.

[2] Tallman, James, Marquino, Wayne., and Alamgir, MD., 2008, "CFD Simulations of Boron Mixing in ESBWR Core Bypass Regions during an Anticipated Transient Without Scram (ATWS) Event", presented at the Proceedings of the 16th International Conference on Nuclear Engineering (ICONE16), May 11-15, 2008, Orlando, Florida, USA.

[3] MFN 07-372 Supplement 1: "Replacement Submittal for Computational Fluid Dynamics (CFD) Model Documentation", February 27, 2008.

[4] Licensing Topical Report: TRACG Application for ESBWR Anticipated Transient Without Scram Analyses, NEDE-33083P Supplement 2, Revision 1, February 2008.

[5] MFN 06-324 – Response to Portion of NRC Request for Additional Information Letter No. 31 Related to ESBWR Design Certification Application – TRACG Application for ESBWR ATWS – RAI Number 21.6-44

[6] MFN 07-372: "Computational Fluid Dynamics (CFD) Model Documentation", August 8, 2007.

APPENDICES INCLUDED:

APPENDIX A: Froude Number Calculations

APPENDIX B: CFD Model Volume vs. Elevation

APPENDIX C: CFD Model Results: Contour Image Sequences for Selected Radial-Axial Planar Cross-Sections of the Model

APPENDIX D: CFD Model Results: Contour Image Sequences for Selected Radial-Tangential Planar Cross-Sections of the Model

DCD IMPACT

No DCD changes will be made in response to this RAI.

No changes to the subject LTR will be made in response to this RAI.

APPENDIX A: Froude Number Calculations

[[

								]]

APPENDIX B: CFD Model Volume vs. Elevation

[[

						]]

APPENDIX C: CFD Model Results: Contour Image Sequences for Selected Radial-Axial Planar Cross-Sections of the Model

[[

]]

APPENDIX D: CFD Model Results: Contour Image Sequences for Selected Radial-Tangential Planar Cross-Sections of the Model

[[

]]

Enclosure 3

MFN 08-659

Response to Portion of NRC Request for

Related to ESBWR Design Certification Application

RAI Number 21.6-44 S01

Affidavit

GE-Hitachi Nuclear Energy Americas LLC

AFFIDAVIT

I, David H. Hinds, state as follows:

(1) I am General Manager, New Units Engineering, GE Hitachi Nuclear Energy ("GEH"), and have been delegated the function of reviewing the information described in paragraph (2) which is sought to be withheld, and have been authorized to apply for its withholding.

(2) The information sought to be withheld is contained in enclosure 1 of GEH's letter, MFN 08-659, Mr. Richard E. Kingston to U.S. Nuclear Energy Commission, entitled "*Response to Portion of NRC Request for Additional Information – Related to ESBWR Design Certification Application – RAI Number 21.6-44 Supplement 1,*" dated September 04, 2008. The proprietary information in enclosure 1, which is entitled "*MFN 08-659 – Response to Portion of NRC Request for Additional Information – Related to ESBWR Design Certification Application – RAI Number 21.6-44 S01 – GEH Proprietary Information,*" is delineated by a [[dotted underline inside double square brackets[3]]]. Figures and large equation objects are identified with double square brackets before and after the object. In each case, the superscript notation [3] refers to Paragraph (3) of this affidavit, which provides the basis for the proprietary determination. Note that the GEH proprietary information in Appendices A and B is identified with a single solid underline. [This sentence is an example.]

(3) In making this application for withholding of proprietary information of which it is the owner or licensee, GEH relies upon the exemption from disclosure set forth in the Freedom of Information Act ("FOIA"), 5 USC Sec. 552(b)(4), and the Trade Secrets Act, 18 USC Sec. 1905, and NRC regulations 10 CFR 9.17(a)(4), and 2.390(a)(4) for "trade secrets" (Exemption 4). The material for which exemption from disclosure is here sought also qualify under the narrower definition of "trade secret", within the meanings assigned to those terms for purposes of FOIA Exemption 4 in, respectively, Critical Mass Energy Project v. Nuclear Regulatory Commission, 975F2d871 (DC Cir. 1992), and Public Citizen Health Research Group v. FDA, 704F2d1280 (DC Cir. 1983).

(4) Some examples of categories of information which fit into the definition of proprietary information are:

a. Information that discloses a process, method, or apparatus, including supporting data and analyses, where prevention of its use by GEH's competitors without license from GEH constitutes a competitive economic advantage over other companies;

b. Information which, if used by a competitor, would reduce his expenditure of resources or improve his competitive position in the design, manufacture, shipment, installation, assurance of quality, or licensing of a similar product;

c. Information which reveals aspects of past, present, or future GEH customer-funded development plans and programs, resulting in potential products to GEH;

d. Information which discloses patentable subject matter for which it may be desirable to obtain patent protection.

The information sought to be withheld is considered to be proprietary for the reasons set forth in paragraphs (4)a. and (4)b. above.

(5) To address 10 CFR 2.390(b)(4), the information sought to be withheld is being submitted to NRC in confidence. The information is of a sort customarily held in confidence by GEH, and is in fact so held. The information sought to be withheld has, to the best of my knowledge and belief, consistently been held in confidence by GEH, no public disclosure has been made, and it is not available in public sources. All disclosures to third parties, including any required transmittals to NRC, have been made, or must be made, pursuant to regulatory provisions or proprietary agreements which provide for maintenance of the information in confidence. Its initial designation as proprietary information, and the subsequent steps taken to prevent its unauthorized disclosure, are as set forth in paragraphs (6) and (7) following.

(6) Initial approval of proprietary treatment of a document is made by the manager of the originating component, the person most likely to be acquainted with the value and sensitivity of the information in relation to industry knowledge, or subject to the terms under which it was licensed to GEH. Access to such documents within GEH is limited on a "need to know" basis.

(7) The procedure for approval of external release of such a document typically requires review by the staff manager, project manager, principal scientist, or other equivalent authority for technical content, competitive effect, and determination of the accuracy of the proprietary designation. Disclosures outside GEH are limited to regulatory bodies, customers, and potential customers, and their agents, suppliers, and licensees, and others with a legitimate need for the information, and then only in accordance with appropriate regulatory provisions or proprietary agreements.

(8) The information identified in paragraph (2) above is classified as proprietary because it contains the results of TRACG analytical models, methods and processes, including computer codes, that GEH has developed and applied to ESBWR Anticipated Transients Without Scram (ATWS) response evaluations. GEH has developed this TRACG code for over fifteen years, at a significant cost. The reporting, evaluation and interpretation of the results, as they relate to the ATWS response evaluations for the ESBWR was achieved at a significant cost to GEH.

(9) Public disclosure of the information sought to be withheld is likely to cause substantial harm to GEH's competitive position and foreclose or reduce the availability of profit-making opportunities. The information is part of GEH's comprehensive BWR safety and technology base, and its commercial value extends beyond the original development cost. The value of the technology base goes beyond the extensive physical database and analytical methodology and includes development of the expertise to determine and apply the appropriate evaluation process. In addition, the technology base includes the value derived from providing analyses done with NRC-approved methods.

The research, development, engineering, analytical and NRC review costs comprise a substantial investment of time and money by GEH.

The precise value of the expertise to devise an evaluation process and apply the correct analytical methodology is difficult to quantify, but it clearly is substantial.

GEH's competitive advantage will be lost if its competitors are able to use the results of the GEH experience to normalize or verify their own process or if they are able to claim an equivalent understanding by demonstrating that they can arrive at the same or similar conclusions.

The value of this information to GEH would be lost if the information were disclosed to the public. Making such information available to competitors without their having been required to undertake a similar expenditure of resources would unfairly provide competitors with a windfall, and deprive GEH of the opportunity to exercise its competitive advantage to seek an adequate return on its large investment in developing and obtaining these very valuable analytical tools.

I declare under penalty of perjury that the foregoing affidavit and the matters stated therein are true and correct to the best of my knowledge, information, and belief.

Executed on this 4th day of September 2008.

David H. Hinds
GE-Hitachi Nuclear Energy Americas LLC